144 (2023) 213204

Contents lists available at ScienceDirect

Biomaterials Advances

journal homepage: www.journals.elsevier.com/materials-science-and-engineering-c

Application of biomimetic surfaces and 3D culture technology to study the role of extracellular matrix interactions in neurite outgrowth and inhibition

K.E. Goncalves [a], S. Phillips [b], D.S.H. Shah [b], D. Athey [b], S.A. Przyborski [a,c,*]

[a] Department of Biosciences, Durham University, South Road, Durham DH1 3LE, UK
[b] Orla Protein Technologies Ltd, (now part of Porvair Sciences Ltd), 73 Clywedog Road East, Wrexham Industrial Estate, Wrexham LL13 9XS, UK
[c] Reprocell Europe Ltd, NETPark Incubator, Thomas Wright Way, Sedgefield TS21 3FD, UK

ARTICLE INFO

Keywords:
3D cell culture
Biomimetic surfaces
Glial scar
Laminin
Y-27632
Neuritogenesis

ABSTRACT

The microenvironment that cells experience during *in vitro* culture can often be far removed from the native environment they are exposed to *in vivo*. To recreate the physiological environment that developing neurites experience *in vivo*, we combine a well-established model of human neurite development with, functionalisation of both 2D and 3D growth substrates with specific extracellular matrix (ECM) derived motifs displayed on engineered scaffold proteins. Functionalisation of growth substrates provides biochemical signals more reminiscent of the *in vivo* environment and the combination of this technology with 3D cell culture techniques, further recapitulates the native cellular environment by providing a more physiologically relevant geometry for neurites to develop. This biomaterials approach was used to study interactions between the ECM and developing neurites, along with the identification of specific motifs able to enhance neuritogenesis within this model. Furthermore, this technology was employed to study the process of neurite inhibition that has a detrimental effect on neuronal connectivity following injury to the central nervous system (CNS). Growth substrates were functionalised with inhibitory peptides released from damaged myelin within the injured spinal cord (Nogo & OMgp). This model was then utilised to study the underlying molecular mechanisms that govern neurite inhibition in addition to potential mechanisms of recovery.

1. Introduction

Neuritogenesis is a developmental process that involves the extension of long cytoskeletal processes from the cell body of the developing neuron and is integral to the proper formation of neuronal connections in the central nervous system (CNS) [1,2]. As with other biological processes, neuritogenesis is highly dependent upon the local microenvironment and many environmental factors influence this process, including, soluble factors, local geometry and extracellular matrix (ECM) interactions [3–5]. Although cell culture *in vitro*, is commonly used to study cellular behavior and to generate model systems, it may not always be representative of the *in vivo* environment, resulting in aberrant cellular behavior [6–9]. For this reason, many attempts have been made to mimic the *in vivo* microenvironment to provide a more physiologically representative *in vitro* environment that better recreates aspects of the native cellular environment.

Developing neurites *in vivo* receive biochemical cues from the ECM that may either promote, inhibit or guide their extension [5,10–15]. Common ECM constituents such as laminin are known to promote neuritogenesis and are often used as standard *in vitro* coatings in many neurite outgrowth models [16–20]. Specific laminin motifs such as "IKVAV" [21–26] and "RNAIAEIIKDI" [27] have been demonstrated to have particular neurite enhancing properties. Extracellular components such as laminin act through integrin receptors to transmit signals inside the cell. In the case of neurite promoting signals, this pathway includes inhibition of Rho A and ROCK, which promotes actin polymerisation and growth cone advancements [5,28–31]. Many of the factors that control neurite development, impact Rho A signaling which exists as a balance, the result of which is thought to be the driving force responsible for neurite dynamics [5].

However, other ECM components such as chondroitin sulphate proteoglycans (CSPGs) and inhibitory molecules released from myelin debris from damaged neurons are inhibitory to neurite generation [32–35]. Following injury to the CNS, such as spinal cord injury (SCI) a sequence of cellular and molecular events occur, initiated by the release of inhibitory CSPGs from reactive astrocytes, along with inhibitory

* Corresponding author at: Department of Biosciences, Durham University, South Road, Durham DH1 3LE, UK.
E-mail address: stefan.przyborski@durham.ac.uk (S.A. Przyborski).

https://doi.org/10.1016/j.bioadv.2022.213204
Received 12 August 2022; Received in revised form 10 November 2022; Accepted 16 November 2022
Available online 21 November 2022

molecules such as oligodendrocyte myelin glycoprotein (OMgp), myelin associated glycoprotein (MAG) and Nogo, released from myelin debris [32–35]. This inhibitory environment that arises post-injury is known as the glial scar and inhibitory molecules such as OMgp, MAG and Nogo are thought to bind to the Nogo receptor (NgR) which in turn leads to Rho A activation, ROCK activation, stabilization of actin filaments, growth cone collapse and neurite retraction [36–49].

Most *in vitro* models rely upon direct adsorption of ECM proteins to culture vessels to mimic the *in vivo* biochemical environment. This has several disadvantages: denaturation; lack of control over the orientation of molecules; and formation of multiple layers of molecules rather than a single monolayer [50]. This can result in some active sites being hidden from cells reducing the functionality and reproducibility of the coating. The cellular impact of ECM-derived molecules is often due to short peptide sequences and immobilising, specific, short active sequences to growth substrates in a controllable manner can be advantageous. Previously, we have demonstrated that peptide motifs can be presented to cells, by use of an engineered variant of outer membrane protein A (OmpA) as a scaffold protein for anchoring the motifs in a structurally intact, correctly orientated and highly functional manner as self-assembled monolayers (SAMs) [51,52]. This "ORLASurf®" technology has been used to generate biomimetic surfaces that can be used in cell culture applications, and have previously been shown to promote neural differentiation [53,54] and cellular adhesion [55], depending upon the ECM-derived motif presented to cells.

In this study, we combine Alvetex® 3D cell culture matrix, a porous polystyrene scaffold, and growth surface functionalisation with OrlaSURF® technology to produce 3D biomimetic surfaces. A well-established and characterised, human pluripotent stem cell-derived model of neuritogenesis [56] was applied to these 3D biomimetic surfaces to study the impact of the ECM and extracellular signaling, on neurite development and inhibition. Specific neurite promoting ECM-derived motifs including those that belong to laminin were identified. Biomimetic and 3D technologies were used to study the process of neurite inhibition that occurs in the glial scar. 2D and 3D growth substrates functionalised with Nogo-66 and OMgp were used to investigate the molecular signaling events that underpin myelin-induced inhibition in the glial scar. Y-27632 a selective ROCK inhibitor and ibuprofen a non-steroidal anti-inflammatory drug (NSAID) inhibitor of Rho A, have both been used to promote neurite outgrowth and functional recovery following SCI, despite the inhibitory environment that forms following injury [57–64]. In this study we use Y-27632 and ibuprofen along with an antagonist of the NgR [65,66] to promote recovery of neurite outgrowth on these inhibitory, biomimetic growth substrates and provide insight into the molecular signaling events involved in glial scar inhibition.

2. Materials & methods

2.1. Cell culture

2.1.1. Maintenance of human pluripotent stem cells

The TERA2.cl.SP12 embryonal carcinoma (EC) pluripotent stem cell line was maintained in Dulbecco's modified Eagle's medium with high glucose (DMEM-HG, ThermoFisher Scientific, Cramlington, UK) supplemented with 10 % heat-treated foetal bovine serum (HT-FBS, ThermoFisher Scientific), 2 mM L-glutamine (ThermoFisher Scientific) and 20 active units of penicillin and streptomycin (ThermoFisher Scientific). Cells were maintained at 37 °C and 5 % CO_2 in a humidified environment in 75 cm^2 culture flasks (BD Falcon, Erembodegem, Belgium) at high confluence to ensure their pluripotent phenotype. Cells were passaged every 3–4 days using acid washed glass beads (ThermoFisher Scientific) to mechanically dislodge cells and subsequently split in a 1:3 ratio and seeded into further 75 cm^2 culture flasks.

2.1.2. Neurosphere formation and induction of neurite outgrowth

EC cells were cultured in suspension as cellular aggregates and differentiated with 0.01 μM EC23 (ReproCELL Europe Ltd., Sedgefield, UK) for 21 days, as described previously [56]. Mature neurospheres were seeded onto biomimetic 2D and 3D surfaces for a further 10-day incubation, during which neurites begin to develop from the neurosphere. Functionalised Alvetex® scaffold 6-well format inserts (ReproCELL Europe Ltd) were prepared by washing for 10 s in 70 % ethanol, followed by two washes in phosphate buffered saline (PBS) (Sigma-Aldrich, Dorset, UK). This rendered the 3D scaffold, hydrophilic, promoting the perfusion of growth medium throughout the culture. Neurospheres were cultured on 2D and 3D surfaces with maintenance medium supplemented with mitotic inhibitors: 1 μM cytosine arabinoside (Sigma-Aldrich), 10 μM 5′fluoro2′deoxyuridine (Sigma-Aldrich) and 10 μM uridine (Sigma-Aldrich). Following the 10-day neurite outgrowth phase of culture, models were fixed in 4 % paraformaldehyde (PFA) (Sigma-Aldrich) prior to immunofluorescence analysis. A range of functionalised 2D and 3D growth substrates were used throughout this study, the details of which can be found in Table 1.

2.1.3. Culture medium supplementation

Throughout this study, a number of small molecules were added to 2D and 3D neurite outgrowth cultures based on inhibitory growth substrates. These molecules were added to cultures during the 10-day neurite outgrowth phase of culture and include: Y-27632 (p160 ROCK inhibitor) (TOCRIS, Bristol, UK), NEP 1-40 (Nogo receptor antagonist) (Sigma-Aldrich) and ibuprofen (NSAID and Rho A inhibitor) (Sigma-Aldrich).

2.2. OrlaSURF® protein engineering, production and surface functionalisation

2.2.1. Orla protein engineering and production

OrlaSURF® proteins were engineered and produced as previously described [36]. Briefly, for small motifs, annealed oligonucleotides encoding the ECM motifs of interest were ligated into an extended loop structure of the engineered OmpA scaffold. For the larger domains such as OMgp, a synthetic gene encoding the domain of interested was ligated to the gene encoding the engineered OmpA scaffold at one of the termini. All the proteins also possess an N-terminal 6xhistidine tag. The fusion proteins were expressed in *E. coli* as inclusion bodies and purified under denaturing conditions using immobilized metal affinity chromatography. The proteins were refolded by dilution *in vitro* and analyzed by SDS PAGE and CD Spectroscopy, see below.

2.2.2. Circular dichroism (CD) spectroscopy

The proteins were diluted to 0.5 mg/mL in ROG-8 Buffer (50 mM TrisHCL, 1 % (*w/v*) n-octylglucoside, 0.1 mM EDTA, pH 8.0). CD spectroscopy was carried out using 0.02 cm pathlength demountable cuvettes in a Jasco J-810 spectropolarimeter. CD was scanned ten times at 25 °C from 250 nm to 180 nm at 20 nm/min scanning speed, averaged, and a buffer blank was subtracted. The data were processed to account for path-length and protein concentration using built-in analysis software (Jasco) and expressed as molar CD (MolCD).

2.2.3. OrlaSURF® protein coating of culture surfaces

Proteins were adsorbed onto polystyrene 6 well plates (Corning) and 6-well format Alvetex® discs. 6 well plates were treated with 3 mL of 0.1 μM protein solution in PBS for 16 h at 4 °C, then washed three times with 3 mL deionized water. Alvetex® discs were treated with 2 mL 0.1 μM protein solution in PBS for 16 h at 4 °C, then washed three times with 2 mL deionized water. 0.1 μM protein solution was used, as this is 100-times greater than the concentration required for saturation of polystyrene (1 nM), to ensure saturation level of coating is consistently reached (Supplementary Fig. 1).

Table 1
Extracellular matrix protein-derived motifs used to create biomimetic 2D and 3D growth substrates.

Sequence	Molecule	Product code
MNYYSNS	Collagen IV	ORLA165
RGDS	Fibronectin	ORLA153
YIGSR	Laminin β1	ORLA163
IKVAV	Laminin α1	ORLA162
IKVSV	Laminin α2	ORLA189
VRWGMQQIQLVV	Laminin α5	ORLA230
DITYVRLKF	Laminin γ1	ORLA236
RNAIAEIIKDI	Laminin γ1	ORLA239
IIHLNLSYNHFTDLHNQLTQYTNLRTLDISNNRLESLPAHLPRSLWNMSAANNNIKLLDKSD TAYQWNLKYLDVSKNMLEKVVLIKNTLRSLEVLNLSSNKLWTVPTNMPSKLHIVDLSNN SLTQILPGTLINLTNLTHLYLHNNKFTFIPDQSFDQLFQLQEITLYNNRW	OMgp	ORLA52
RIYKGVIQAIQKSDEGHPFRAYLESEVAISEELVQKYSNSALGHVNSTIKELRRLFL VDDLVDSLK	Nogo-66	ORLA51

A table containing details of each ECM protein-derived motif used in this study to investigate the role of extracellular signals in neurite development and inhibition.

2.3. Immunofluorescence analysis of 2D and 3D neurite outgrowth models

Fixed, 2D and 3D neurite outgrowth models were permeabilized in 0.1 % Triton X-100 (Sigma-Aldrich) 3D for 20 min and 2D for 10 min. 3D scaffolds were then blocked for 30 min and 2D cultures blocked for 60 min in a blocking solution consisting of: 1 % normal goat serum (NGS, Sigma-Aldrich) and 0.01 % Tween (Sigma-Aldrich) in PBS. Cultures were incubated with the primary antibody (anti- β-III-tubulin (Cambridge Bioscience, Cambridge, UK)) diluted in blocking buffer for 1 (2D) or 2 (3D) hours at room temperature. Both 2D and 3D samples were then washed three times for 10 min in blocking buffer and incubated with the secondary antibody (Alexafluor® anti-rabbit 488 (ThermoFisher)) diluted in blocking buffer with the addition of the nuclear dye Hoechst 33342 (ThermoFisher Scientific) for 1 h at room temperature. Samples were then washed 3 times for 10 min in blocking buffer and 3D scaffolds were mounted on microscope slides with Vectashield anti-fade mounting medium (Vector Laboratories, Peterbrough, UK), whilst 2D samples were stored in PBS prior to imaging. Confocal images were obtained using the Zeiss 880 confocal microscope with Zen software.

2.4. Image analysis

Image J software was used to quantify neurite outgrowth by calibrating the scale of the software and tracing individual neurites using the freehand line tool. A sampling method described previously [56] was used to quantify neurite outgrowth from 2D cultures. This involved the use of grid overlay and the selection of 3 squares at random for quantification. We have previously demonstrated this to be both an efficient and accurate means of quantification that did not significantly differ from measuring each individual neurite in turn [56]. Each neurite was traced from the tip of the growth cone to the perikaryon, which in this case, is located in the central neurosphere mass, providing an accurate method of quantification with minimal branching and crossing. To normalize to neurosphere size, we also present 2D neurite outgrowth data as neurite density whereby the number of neurites per μm of neurosphere circumference has been calculated by dividing the total number of neurites by the circumference of the neurosphere.

As for 3D cultures, scaffolds were prepared for wholemount microscopy and immunostained for pan-neuronal marker TUJ-1, they were then imaged from the underside to visualize neurite penetration. As described previously [56], individual neurites were then able to be counted using the multipoint tool in Image J software and expressed as number of neurites penetrating the scaffold in each treatment condition.

2.5. Statistical analysis

GraphPad Prism v7 was used to assess the statistical significance of results and in all cases an ANOVA was conducted to determine significance, which is depicted graphically for each data set with * = $p < 0.05$, ** = $p < 0.01$, *** = $p < 0.001$, **** = $p < 0.0001$.

3. Results

3.1. Protein production and QA

Several types of functional protein motifs were engineered using modified version of the *E. coli* protein OmpA and presented on the surface of cell culture growth substrates in a manner optimal to their structure, as depicted by the schematic illustration Fig. 1A. A range of ECM associated motifs and domains were used throughout the study and are specified in Table 1, including domains derived from laminins, collagens and glial scar associated inhibitory molecules. The OrlaSURF® fusion proteins described in this study were expressed in *E. coli* in 1 L shaken flask cultures and purified as detailed in materials and methods. SDS PAGE analysis showed that the proteins were > 95 % homogenous (Supplementary Fig. 2) and a scaffold protein that is identical to the test proteins but has a FLAG epitope was used as negative control.

The refolding of denatured proteins *in vitro* can result in large populations of misfolded proteins. Normally such proteins tend to precipitate and can be removed by centrifugation. However, there may be some misfolded states that retain solubility but lack function. Circular dichroism (CD) spectroscopy can be employed to determine that the majority of the population has the expected secondary structure and is routinely used as a Quality Assurance (QA) technique. To exemplify this, Fig. 1B demonstrates the CD spectra of three of the proteins used in this study. The engineered OmpA (ORLA154) is almost entirely a beta-barrel structure and shows a typical trough at 215 nm (Fig. 1Bb). The small motif insertions of laminin γ do not impart significant structural differences on the Omp molecule and the spectra are similar to the control. The larger OMgp domain is predicted to have two short α-helices in its structure and this is reflected in the different CD spectrum from the ORLA52 (OMgp) protein. These data show that the majority of molecules are refolded correctly *in vitro*, suggesting retention of functionality.

3.2. Application of 2D and 3D biomimetic surfaces to investigate the role of ECM-derived motifs in neurite development

Neurospheres matured for 21 days were cultured on 2D (Fig. 2Aa-d) and 3D (Fig. 2Ae-l) surfaces functionalised with: FLAG (epitope control), MNYYSNS motif of collagen IV, RGDS motif of fibronectin or YIGSR motif of laminin β1. In 2D cultures neurites radiate from the central cellular mass. Few radiating neurites are visible from neurospheres cultured on control FLAG surfaces, whereas denser neurite outgrowth is visible from neurospheres cultured on surfaces functionalised with ECM–derived motifs. Neurites that developed on Collagen IV MNYYSNS

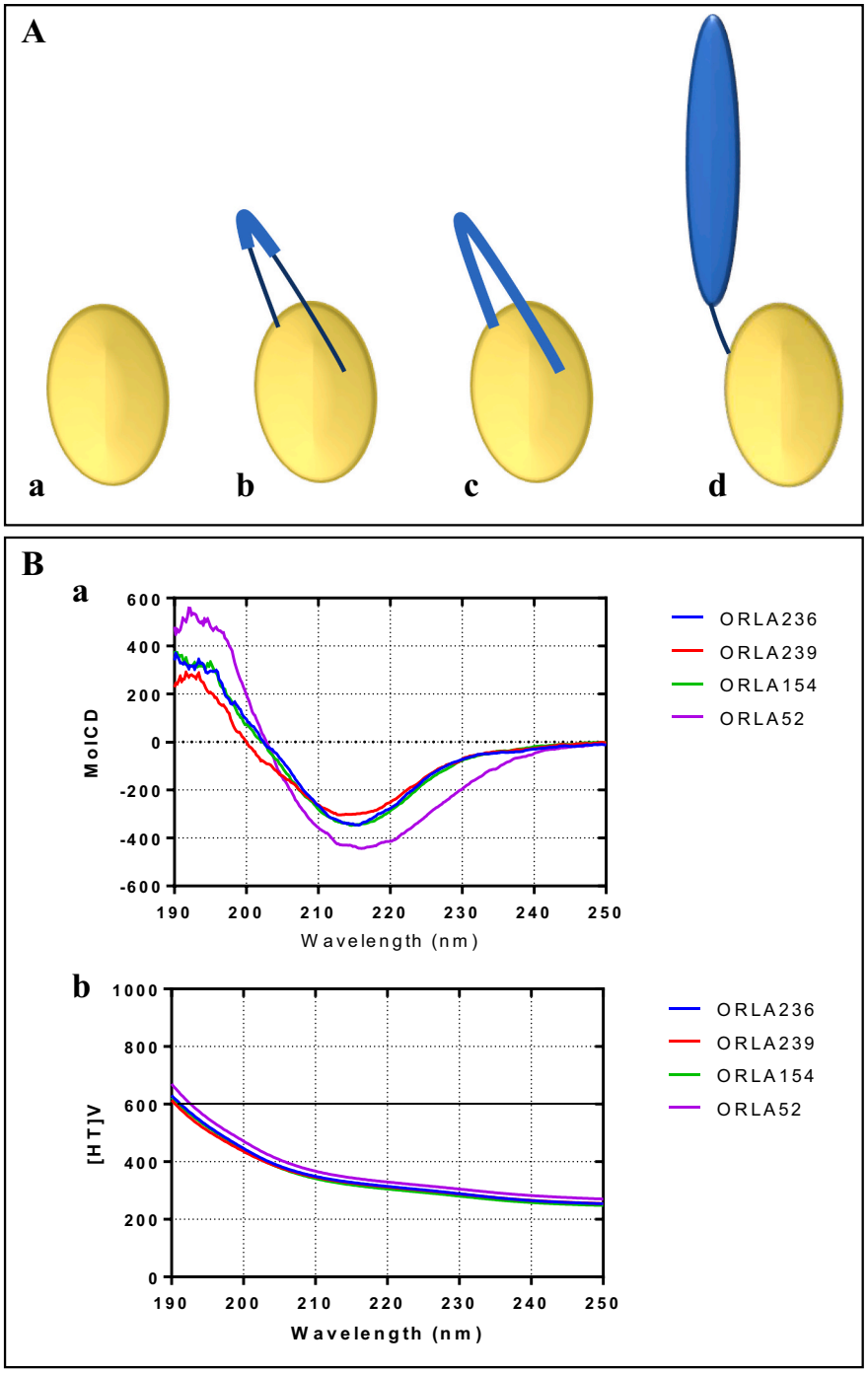

Fig. 1. Structure and characterization of engineered proteins.
(A) Representation of the biologically active motifs and domains (shown in blue). All of the proteins are based on a modified version of the *E. coli* protein OmpA (Aa, shown in yellow), functional motifs and domains have been engineered into the protein in multiple ways allowing optimum presentation of the active sequences to the cells. Small motifs derived from collagen, fibronectin or laminin were inserted into a large loop (Ab). Nogo-66 sequence replaced the large loop (Ac). OMgp was created as an N-terminal fusion (Ad). (Ba) The CD data from 190 to 250 nm are plotted. Below 190 nm the high-tension voltage (HT[V], Bb) is above 600 and indicates that the detector is saturated, and data become unreliable. Key: ORLA52 – amino acids 57–228 (from Uniprot P23515) of OMgp fused to Omp N-terminus; ORLA236 – DITYRLKF motif of human laminin γ-1 in Omp loop; ORLA239 – RNIAEIIKDI motif of mouse laminin γ-1 in Omp loop; ORLA154 – control Omp with no fused effector motifs or domains.

sequence are shorter than those on YIGSR, and neurite outgrowth on RGDS appears to be less uniform than on the other conditions. These visual observations are confirmed by quantification of neurite number, density (normalized to neurosphere size) and length (Fig. 2B–D). Fibronectin and laminin β1 motifs significantly enhance neurite number, density and length compared with FLAG epitope control, with YIGSR of Laminin β1 showing the greatest enhancement.

In 3D culture, neurospheres remain on top of the scaffold whilst neurites penetrate through the depth of the 3D material (200 μm) and are visible from the underside of the scaffold. Significant neurite outgrowth can be observed from the bottom of scaffolds functionalised with both RGDS and YIGSR but little outgrowth is visible on MNYYSNS or FLAG functionalized scaffolds. Quantification of neurite outgrowth from 3D scaffolds (Fig. 2E) revealed that fibronectin RGDS and laminin β1 YIGS cause a significant enhancement compared to FLAG, uncoated and MNYYSNS. Since the laminin β1 YIGSR motif was found to have the greatest impact in both 2D and 3D neuritogenesis, the role of laminin in neurite development was investigated further.

3.3. Use of 2D and 3D biomimetic surfaces to determine the role of laminin in neurite development

In order to better understand the relationship between laminin and neuritogenesis a dose response was performed, which in this case investigated the effect of the surface density of a laminin-derived motif on neurite outgrowth in 2D culture. The effect of differing surface

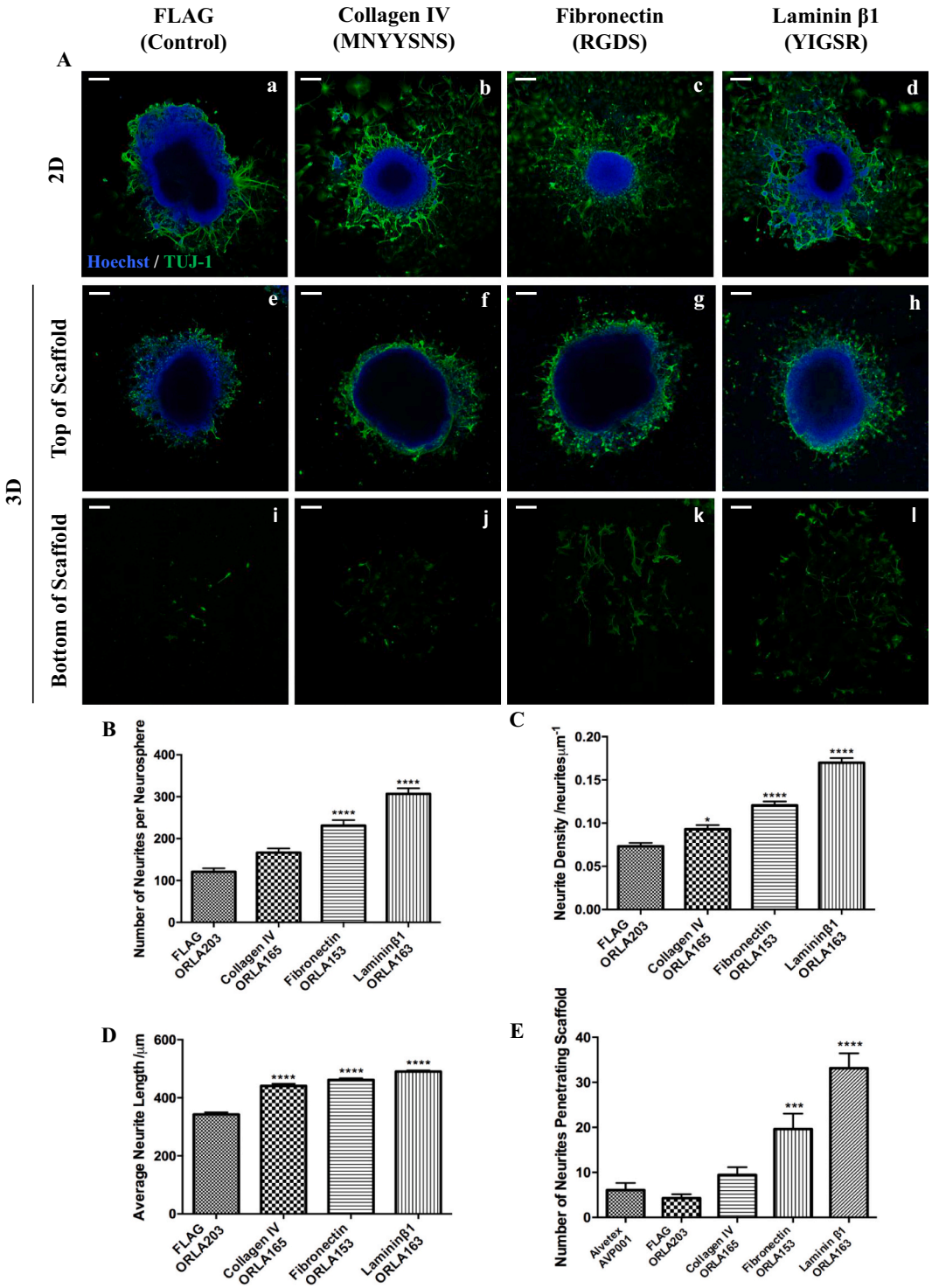

Fig. 2. Cellular interaction with ECM components can induce neurite outgrowth in 2D and 3D culture.
Representative confocal images (A) of human pluripotent stem cell-derived neurospheres cultured on biomimetic 2D (Aa-d) or 3D (Ae-l) surfaces for 10 days. The pan-neuronal marker TUJ-1 stained green highlights neurites, whereas, nuclei are stained by hoechst in blue. Neurospheres were cultured on surfaces coated with the FLAG missense control peptide (Aa,e,i), the "MNYYSNS" motif of collagen IV (Ab,f,j), "RGDS" of fibronectin (Ac,g,k) or "YIGSR" of laminin (Ad,h,l). The number of neurites per neurosphere (B) (data represent mean ± SEM, $n = 33–45$) was quantified from 2D cultures and this was normalized to neurosphere size and expressed as neurite density (C) (data represent mean ± SEM, n = 33–45). The average neurite length (D) (data represent mean ± SEM, $n = 476–1340$) was also quantified from 2D cultures and penetration of neurite (D) (data represent mean ± SEM, $n = 13–15$) through the scaffold was measured from 3D cultures. Scale bars: 200 μm. * = $p \leq 0.05$, ** = $p \leq 0.01$, *** = $p \leq 0.001$, **** = $p \leq 0.0001$.

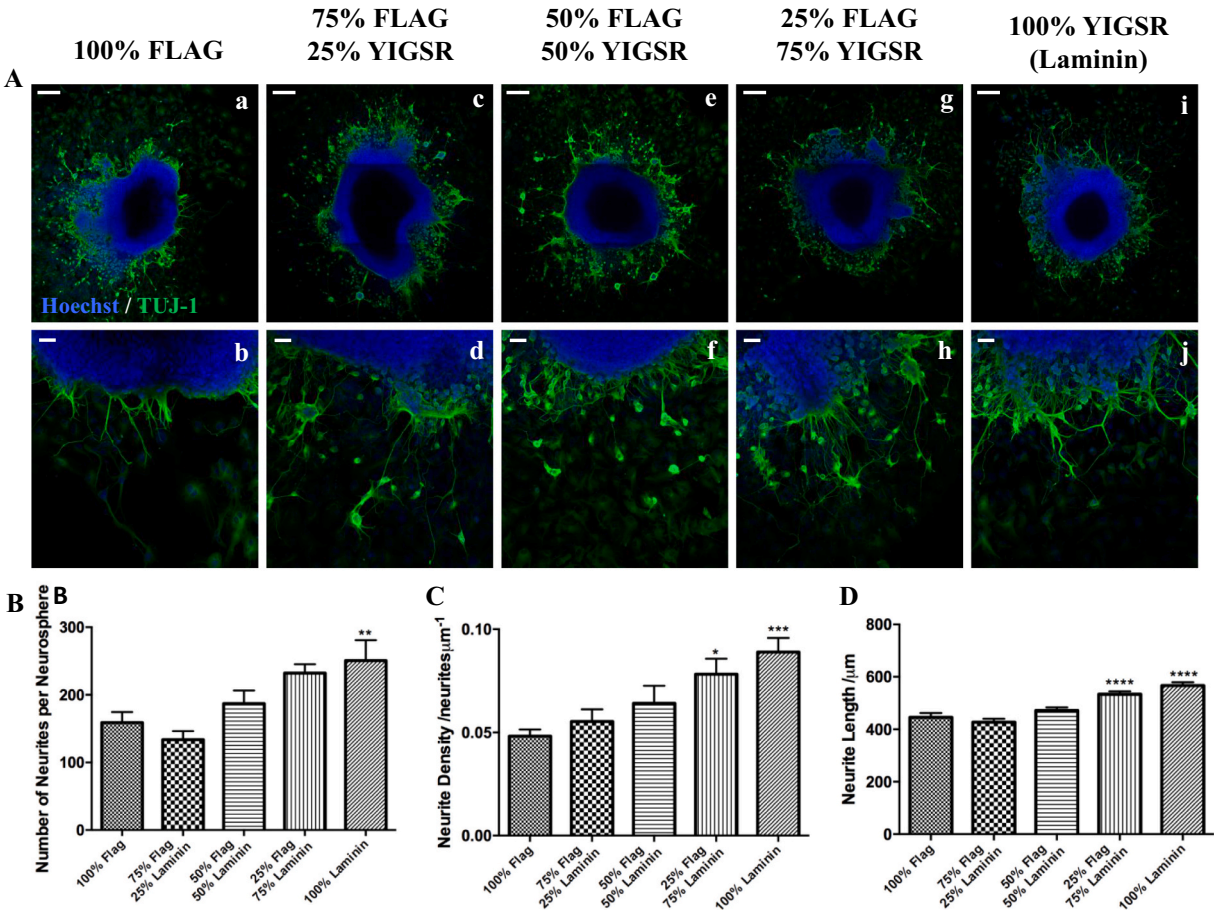

Fig. 3. The laminin "YIGSR" motif enhances neurite outgrowth in a dose dependent manner in 2D culture.
Representative confocal images (A) of neurospheres cultured on 2D surfaces functionalised with increasing "YIGSR" content mixed with the control peptide, FLAG. Neurites are positive for TUJ-1 (green) and nuclei are stained blue. The number of neurites per neurosphere (B) (data represent mean ± SEM, $n = 18$), neurite density (C) (data represent mean ± SEM, n = 18) and average length of neurites (D) (data represent mean ± SEM, $n = 224–419$) were quantified from 2D neurite outgrowth models. Scale bars: 200 µm. * = $p \leq 0.05$, ** = $p \leq 0.01$, *** = $p \leq 0.001$, **** = $p \leq 0.0001$.

densities the laminin β1 YIGSR motif was investigated by measuring neuritogenesis on 2D surfaces coated with mixtures of FLAG-control protein and ORLA163 protein (YIGSR) in different ratios (Fig. 3A). Neurite number, density and length increased with increasing YIGSR content. 100 % YIGSR gave the most significant enhancement of neurite outgrowth (Fig. 3B–D). These results suggest that the YIGSR laminin β1-derived motif enhances neurite outgrowth in a dose dependent manner.

Other laminin-derived motifs, IKVAV, IKVSV, RNAIAEIKDI, VRWGMQQIQLVV and DITYVRLKF were tested on 2D (Fig. 4Aa-c, h-j) and 3D (Fig. 4Ae-g, k-m) surfaces alongside YIGSR and the FLAG control. IKVAV, and YIGSR induced the growth of longer neurites in 2D culture (Fig. 4B). Whereas growth on IKVAV, IKVSV, RNAIAEIKDI 3D substrates resulted in greater neurite penetration through 3D scaffolds and VRWGMQQIQLVV and DITYVRLKF did not perform better than FLAG control (Fig. 4D).

3.4. Application of 2D and 3D biomimetic surfaces to investigate myelin-induced neurite inhibition and methods of recovery

In order to study the molecular mecanisms that underpin myelin-induced inhibitiron of neurite re-growth in the injured spinal cord, we funtionalised both 2D and 3D growth substrates with sequences derived from inhibitory molecules found in the glial scar including OMgp and the 66 amino-acid effector loop of Nogo (Nogo-66). Fig. 5 demonstrates the results of the neuritogenesis assay on surfaces coated with either protein alone or a 50:50 mixture of Nogo-66 and OMgp compared to surfaces coated with FLAG-epitope control. Both the OMgp and Nogo-66 are highly inhibitory compared to the control as indicated by the reduced neurite density (Fig. 5B) and shorter neurite length (Fig. 5C) when cultured in 2D (Fig. 5Aa-h) and reduced penetration through the scaffold in 3D culture (Fig. 5Ai-p, D). The greatest inhibitory effect on neurite length, density and penetration is seen on substrates functionalized with a 50:50 mixture of OMgp and Nogo-66, suggesting an additive effect.

Recovery of glial-scar induced neurite inhibition can be achieved by blocking NgR and its downstream events, including Rho A and ROCK-mediated signaling [58,64–69]. Here, we tested the ability of the NgR antagonist peptide, NEP 1-40 and two small molecule inhibitors Y-27632 and ibuprofen (inhibitors of ROCK and Rho A respectively) to reverse the effects of OMgp and/or Nogo-66 (Fig. 6). Neurospheres were cultured on 2D surfaces functionalised with either: FLAG-epitope, Nogo-66, OMgp or a 50:50 OMgp:Nogo-66 mixture. The addition of 10 µM Y-27632, 100 µM ibuprofen or 1 µM peptide NEP 1-40 to the culture medium reversed the inhibitory effects of OMgp and Nogo-66 in our model system, resulting in significant neurite outgrowth, with extremely densely packed neurites and fascicles radiating from each neurosphere despite the inhibitory stimulus (Fig. 6A). Ibuprofen and NEP 1-40 recovered neurite density to the level on FLAG-epitope surfaces whereas Y-27632 treatment resulted in a significant increase (Fig. 6B) indicating a stimulatory effect on neurite outgrowth. Although the antagonists of the NgR/RhoA/ROCK signaling pathway reversed the inhibitory effect of Nogo and OMgp on neurite number and density, their

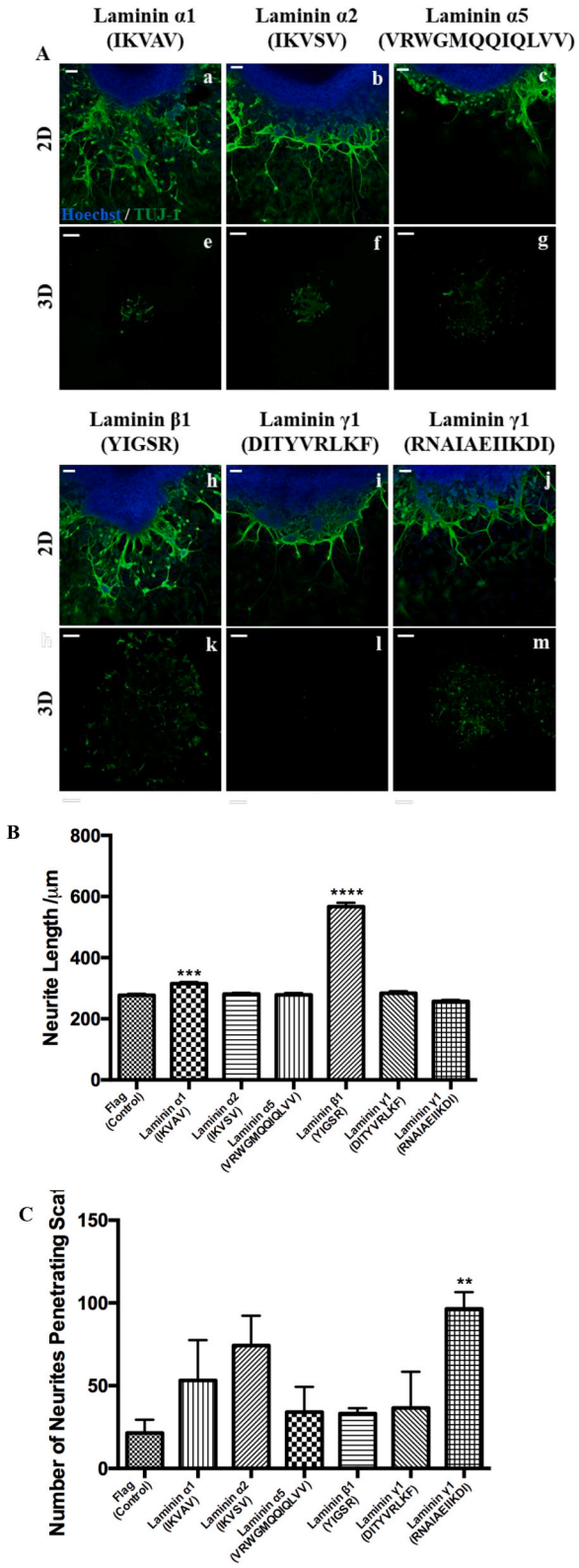

Fig. 4. Enhancement of neurite outgrowth in 2D and 3D culture by specific laminin-motifs.
Representative confocal images (A) of neurospheres cultured on 2D (Aa-c, h-j) and 3D (Ae-g, k-m) functionalised substrates coated with a range of laminin motifs. 3D neurite outgrowth is visualized from neurite penetration through the bottom of the scaffold. Neurite outgrowth is highlighted by positive staining for TUJ-1 (green) and nuclei are stained in blue. Quantification of neurite length (B) (data represent mean ± SEM, n = 184–354) from 2D neurite outgrowth models and neurite penetration through the scaffold (c) (data represent mean ± SEM, $n = 9$) from 3D neurite outgrowth models. Scale bars: 2D images: 50 μm 3D images: 200 μm. * = $p \leq 0.05$, ** = $p \leq 0.01$, *** = $p \leq 0.001$, **** = $p \leq 0.0001$.

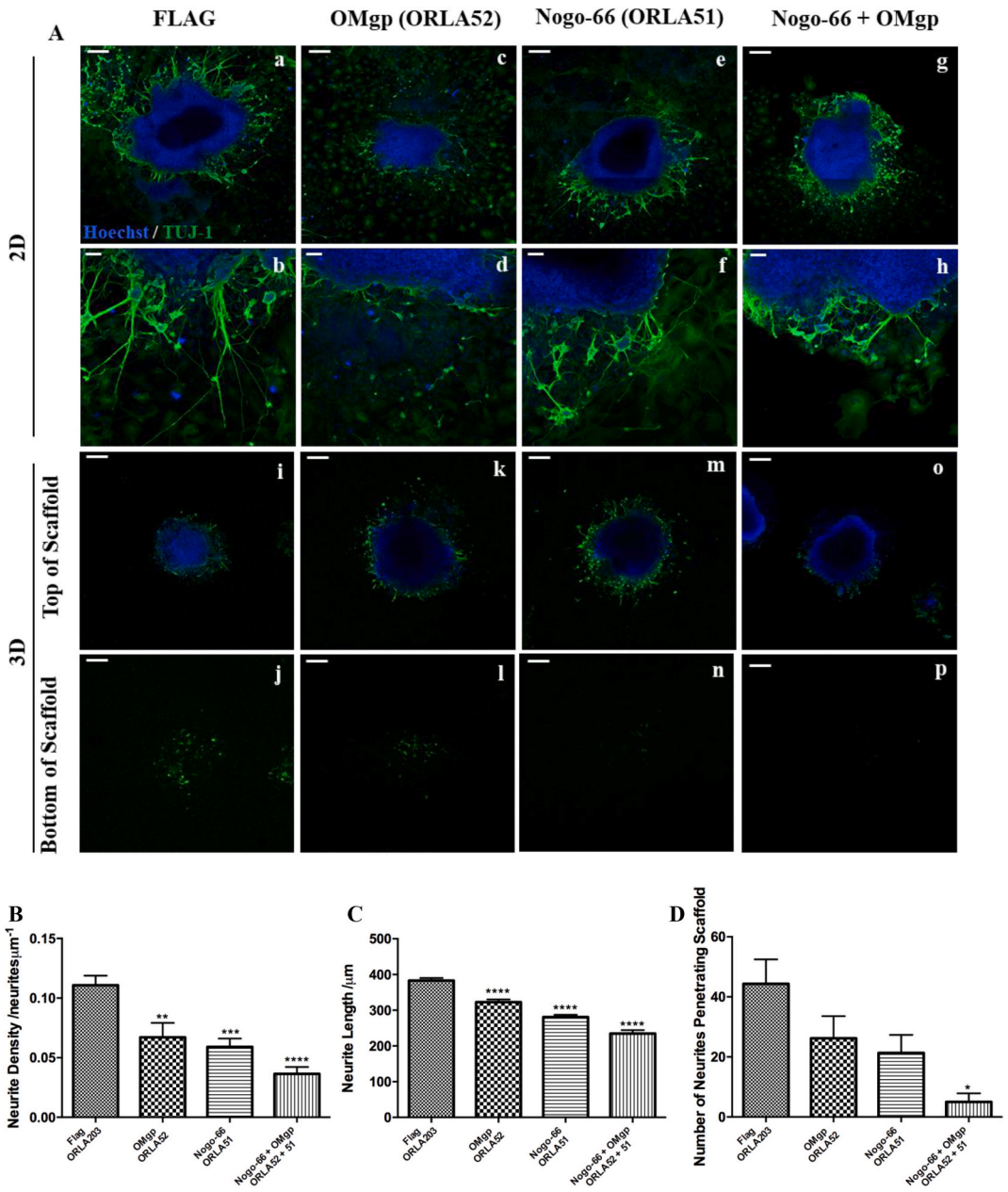

Fig. 5. 2D and 3D biomaterials functionalised with inhibitory molecules from the glial scar induce neurite inhibition.
Representative confocal images (A) of neurospheres cultured on 2D (Aa-h) and 3D (Ai-p) surfaces functionalised with a control peptide (Aa,b,i,j), OMgp (Ac,d,k,l), Nogo (Ae,f,m,n) or a 50:50 mixture of Nogo and OMgp (Ag,h,o,p). Neurite outgrowth is highlighted in green through positive staining of the pan-neuronal marker TUJ-1 and nuclei are stained blue. Quantification of neurite density (B) (data represent mean ± SEM, n = 9) and length (C) (data represent mean ± SEM, n = 118–492) describes 2D neurite outgrowth whilst neurite penetration (D) (data represent mean ± SEM, n = 5–6) describes neurite outgrowth in 3D culture. Scale bars: Aa,c,e,g,i-p: 200 µm Ab,d,f,h,: 50 µm. * = $p \leq 0.05$, ** = $p \leq 0.01$, *** = $p \leq 0.001$, **** = $p \leq 0.0001$.

effect on neurite length was less marked (Fig. 6C). If anything, there appears to be a slight inhibitory effect of these compounds when the data on the FLAG-control surfaces is considered.

In 3D culture (Fig. 7A), very few neurites are visible from the underside of scaffolds cultured on inhibitory 3D growth substrates in the absence of medium supplementation. Supplementation of the culture medium with Y-27632 resulted in significant neurite outgrowth and a large interconnected network of neurites could be seen from the bottom view of scaffolds. This stimulatory effect was also apparent on the control FLAG-epitope surfaces. Ibuprofen overcame the inhibitory effect on Nogo but not on OMgp surfaces whereas NEP 1-40 was able to reverse inhibition on both Nogo and OMgp (Fig. 7B).

4. Discussion

Biomimetic surfaces combined with 3D cell culture technology aim to provide a more physiologically relevant *in vitro* microenvironment than traditional tissue culture techniques, by recapitulating the biochemical composition of the ECM along with the 3D cellular geometry associated with cell and tissue development *in vivo* [3,4,6]. 2D and 3D functionalised growth substrates were used to identify specific ECM-derived motifs capable of promoting neuritogenesis. Unsurprisingly, the laminin "YIGSR" motif was found to promote neurite outgrowth in both 2D and 3D culture to a greater extent than collagen IV's "MNYYSNS" or "RGDS" of fibronectin. "YIGSR" has previously been documented to promote neuritogenesis and laminin has long since formed the basis of *in*

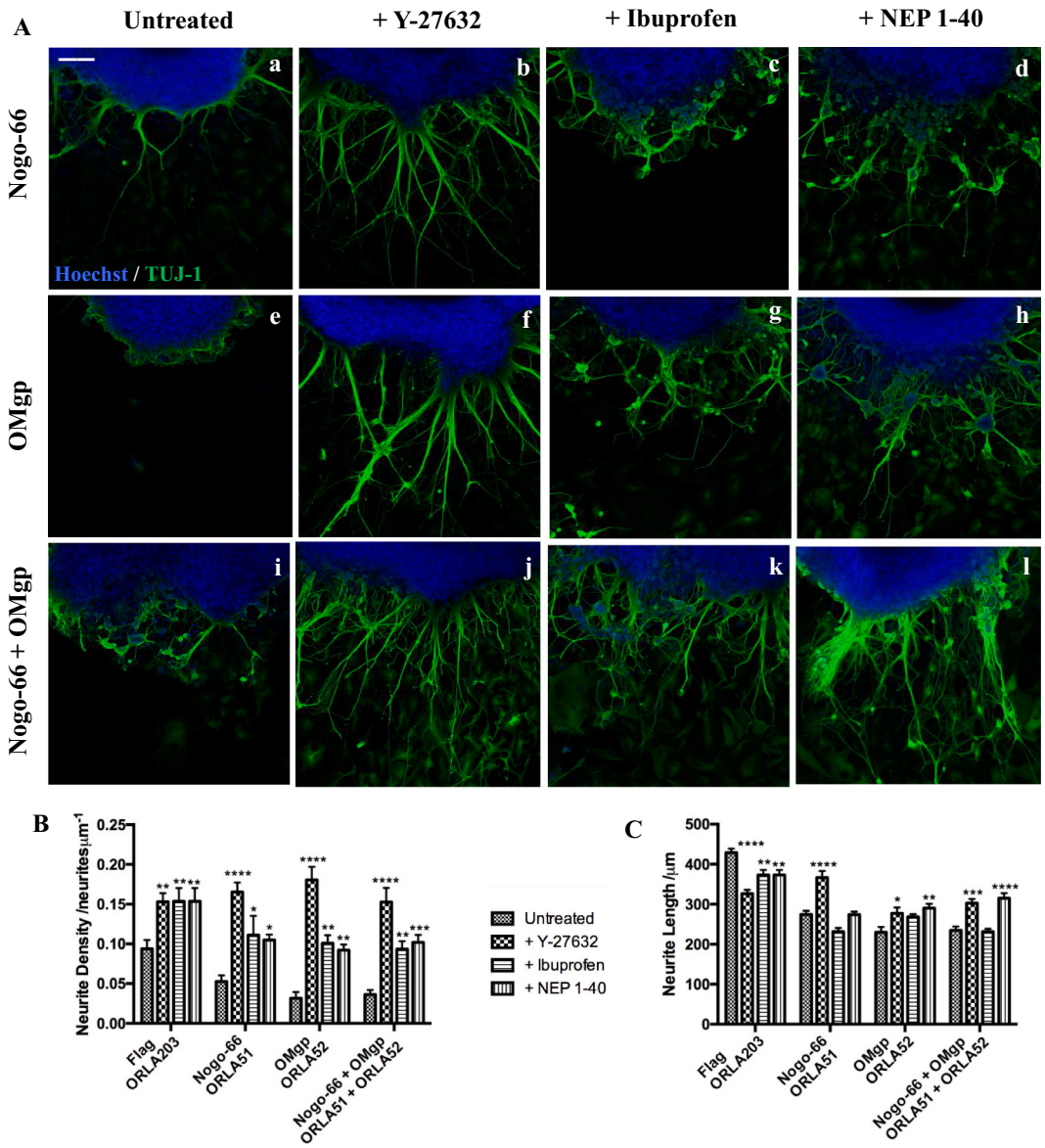

Fig. 6. Inhibition of the Nogo receptor and its downstream signaling events, restore neurite outgrowth on 2D inhibitory surfaces.
Representative confocal images (A) of neurospheres cultured on inhibitory 2D surfaces functionalised with Nogo (Aa-d), OMgp (Ae-h) or a 50:50 mix of the two peptides (Ai-l). Cultures also received medium supplementation with 15 μM Y-27632 (a selective ROCK inhibitor) (Ab,f,j), 500 μM ibuprofen (inhibitor of Rho A) (Ac, g,k) or 1 μM NEP 1–40 (Nogo receptor antagonist peptide) (Ad,h,l). TUJ-1 expression (green) highlights neurite outgrowth and nuclei, stained blue, remain in the central body of the neurosphere. Quantification of the neurite density (B) (data represent mean ± SEM, $n = 15$) and neurite length (C) (data represent mean ± SEM, $n = 45$–391). Scale bars: 100 μm. * = $p \leq 0.05$, ** = $p \leq 0.01$, *** = $p \leq 0.001$, **** = $p \leq 0.0001$.

vitro neuritogenesis models [70–72]. For this reason, the study focused upon the neurite outgrowth promoting effects of laminin and determined specific laminin-derived motifs responsible for its neurite promoting properties.

The "YIGSR" motif of laminin β1 enhanced neurite outgrowth in a dose dependent manner, suggesting an active effect upon neurite outgrowth, and further confirming that the motif is in fact responsible for the enhancement of neurite outgrowth observed *in vitro*. Certain laminin-derived motifs such as "IKVAV", "IKVSV" and "YIGSR" were found to enhance neuritogenesis in 2D and 3D culture. This is supported by evidence previously described throughout the literature as "IKVAV" and "IKVSV" have both been shown to induce neurite development in several model systems, potentially through a β1 integrin dependent mechanism [21–23,73–77]. The larger laminin-derived sequence "VRWGMQQIQLVV" from the α5 chain was found to inhibit certain aspects of neurite outgrowth and have no effect upon others. This sequence is derived from the LG4 domain of the α5 chain, which has previously been shown to enhance neurite outgrowth *in vitro* [78]. However, the α5 chain is expressed at low levels in the adult brain and is mostly expressed in other tissues including: bone marrow, pancreas, lung and heart [79]. This could explain the lack of α5 involvement in neuritogenesis and why the "VRWGMQQIQLVV" seemed to have little impact upon neurite outgrowth in this system. Both "DITYVRLKF" and "RNAIAEIIKDI" from the γ1 laminin chain were also screened for their ability to induce neuritogenesis. Both sequences had previously been implicated in cell adhesion and neurite outgrowth *in vitro* [80], however, "DITYVRLKF" was found to have little impact on neurite outgrowth but "RNAIAEIIKDI" was found to enhance neurite outgrowth, particularly in 3D culture.

This method of presentation of ECM-derived motifs to cells within the context of biomimetic surfaces offers several advantages over traditional ECM adsorption coating including a reduction in the use of

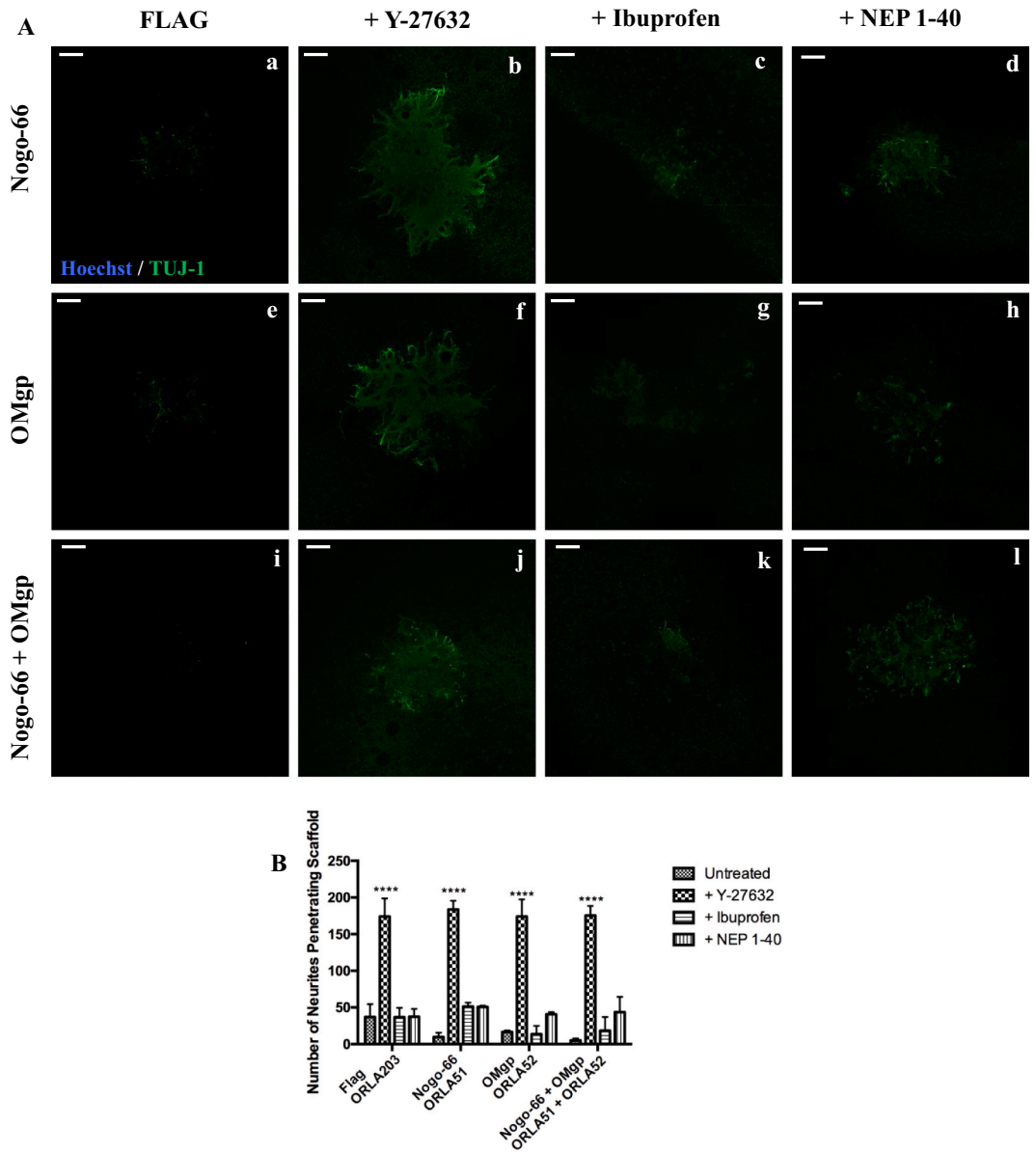

Fig. 7. Inhibition of the Nogo receptor and its downstream signaling events, restore neurite outgrowth on 3D inhibitory surfaces.
Representative confocal images (A) of neurite outgrowth from neurospheres cultured in 3D on top of Alvetex® scaffold functionalised with Nogo (Aa-d), OMgp (Ae-h) or a 50:50 mixture of the two peptides (Ai-l). Culture medium was also supplemented with 15 μM Y-27632 (a selective ROCK inhibitor) (Ab,f,j), 500 μM ibuprofen (inhibitor of Rho A) (Ac,g,k) or 1 μM NEP 1-40 (nogo receptor antagonist peptide) (Ad,h,l). TUJ-1 positive neurites (green) visibly penetrate the depth of the 3D material, represented here as the bottom view of the scaffold. Quantification of the number of neurites that penetrate the 3D material (B) (data represent mean ± SEM, $n = 9$). Scale bars: 200 μm. * = $p \leq 0.05$, ** = $p \leq 0.01$, *** = $p \leq 0.001$, **** = $p \leq 0.0001$.

animal-derived products, excellent reproducibility, good availability of active sites and precise orientation of motifs. In this study we have demonstrated that functionalisation of growth substrates with specific laminin-derived motifs displayed in an accessible orientation on a scaffold protein can induce neuritogenesis *in vitro*. This has several advantages such as providing a cost-effective, animal product free, standardized, reproducible growth surface suitable for industrial applications including screening potential neurotoxic compounds.

In addition to describing the role of the ECM in neurite promotion, this study also examined the ability of 2D and 3D growth substrates functionalised with inhibitory molecules from the glial scar, to induce neurite retraction and inhibition of growth. The glial scar forms following SCI and many inhibitory mechanisms contribute the lack of neuronal regeneration within the glial scar and prevent functional recovery following injury [33–35,81,82]. One of the inhibitory mechanisms implicated in glial scar signaling, involves the binding of inhibitory molecules from myelin debris released from damaged neurons, to receptors including the NgR. OMgp and Nogo-66 are myelin-associated inhibitory molecules that bind to NgR, which acts through co-receptors (p75 [40,46,83], TROY [45,49] and LINGO-1 [42,49,84]) to induce growth cone collapse and neurite retraction through activation of downstream Rho A and ROCK.

This study describes the use of functionalised 2D and 3D surfaces to elucidate the molecular signaling events that underpin myelin-induced neurite inhibition in the glial scar. We demonstrate that both 2D and 3D growth substrates functionalised with Nogo-66 and OMgp result in neurite inhibition. This culture system models the process of myelin-induced neurite inhibition that is involved in the formation of the glial scar. This has many applications including screening potential candidates that may be able to overcome this inhibitory response, along with

supporting investigations into the underpinning molecular signaling pathways involved in the inhibitory response.

OMgp and Nogo-66 are both known to activate the NgR which in turn activates Rho A and ROCK resulting in growth cone collapse and neurite inhibition [36–38,48]. For this reason, an antagonist of the NgR, NEP 1-40 [65,66] was added to the culture medium of inhibition models to intervene at the receptor stage of signaling. Inhibition models were also supplemented with the selective ROCK inhibitor, Y-27632 and ibuprofen, an inhibitor of Rho A, to intervene in signaling events downstream of the NgR. All of these compounds have previously been demonstrated to restore neurite growth in *in vitro* and *in vivo* models of SCI [58,59,61–63,68,69,85–90]. NEP 1-40 mimics the first 40 amino acids of Nogo-66 and blocks receptor-ligand binding [65,66]. In this study NEP 1-40 was found to overcome inhibition in terms of neurite density and 3D growth but not inhibition in neurite length mediated by OMgp and Nogo-66. This suggests that OMgp and Nogo-66-mediated inhibition in this system acts through the expected signaling channels, depending upon NgR activation. However, NEP 1-40 did not restore inhibition of neurite length, which may be impacted by another, unknown mechanism of inhibition. Inhibition of ROCK by Y-27632 enhanced neurite outgrowth in many cases, with significant neuritogenesis being observed in both 2D and 3D cultures. Supplementation with this molecule rescued neurite density and 3D outgrowth, however, had variable results upon neurite length. Similarly, inhibition of Rho A by ibuprofen, was found to recover neurite number and density but have variable results upon 3D neurite outgrowth and neurite length in 3D. This may suggest that neurite length is controlled by a different mechanism independent of Rho A and ROCK, compared with neurite number and density.

5. Conclusions

In this study we have combined OrlaSURF® protein surface technology and Alvetex® 3D cell culture technology to provide a more physiologically relevant microenvironment to study a well-established model of the human neuritogenesis developmental process. This has allowed for the identification of specific motifs responsible for the positive effects of laminin upon neurite development. Furthermore, we have also developed biomimetic non-permissive growth surfaces to model myelin-induced inhibition, a process that inhibits neural regeneration following SCI. This model can be used to further elucidate molecular signaling involved in the induction of neurite inhibition or have applications in screening compounds for their ability to overcome myelin-induced inhibition.

In conclusion, we present a novel application of OrlaSURF® protein technology to better understand the microenvironmental influences that underpin neurite outgrowth and inhibition within the CNS. The combination of a biomimetic, functionalized growth substrate with 3D cell culture technology provides a platform to better understand how physical and chemical cues integrate to influence neurite growth dynamics in developmental and injured scenarios.

CRediT authorship contribution statement

KEG, SP, DSHS, DA and SP helped develop the initial concepts behind the study. KEG was largely responsible for the experimental plan and initial drafting the manuscript with input SP, DSHS and *SP*. KEG, DSHS and SP performed the experimental work. All co-authors reviewed and approved the final manuscript. SP is the Principal Investigator and corresponding author.

Funding

This study was supported by a BBSRC CASE training studentship (KG; BB/K011413/1).

Declaration of competing interest

Sion Phillips, Deepan Shah and Dale Athey were employed by Orla Protein Technologies at the time the research was conducted. Orla Protein Technologies has since been sold in 2018 to Porvair Sciences Ltd.

Deepan Shah declares that he has carried out consultancy for the new owners but is not under contract to do so in future.

Data availability

No data was used for the research described in the article.

Appendix A. Supplementary data

Supplementary data to this article can be found online at https://doi.org/10.1016/j.bioadv.2022.213204.

References

[1] J.S. Da Silva, C.G. Dotti, Breaking the neuronal sphere: regulation of the actin cytoskeleton in neuritogenesis, Nat. Rev. Neurosci. 3 (2002) 694–704, https://doi.org/10.1038/nrn918.
[2] S.A. Bennison, S.M. Blazejewski, T.H. Smith, K. Toyo-oka, Protein kinases: master regulators of neuritogenesis and therapeutic targets for axon regeneration, Cell. Mol. Life Sci. 77 (2020) 1511–1530, https://doi.org/10.1007/s00018-019-03336-6.
[3] K.M. Yamada, E. Cukierman, Modeling tissue morphogenesis and cancer in 3D, Cell 130 (2007) 601–610, https://doi.org/10.1016/j.cell.2007.08.006.
[4] E. Cukierman, R. Pankov, D.R. Stevens, K.M. Yamada, Taking cell-matrix adhesions to the third dimension, Science (80-.) 294 (2001) 1708 LP–1712, http://science.sciencemag.org/content/294/5547/1708.abstract.
[5] J.P. Myers, M. Santiago-Medina, T.M. Gomez, Regulation of axonal outgrowth and pathfinding by integrin-ECM interactions, Dev. Neurobiol. 71 (2011) 901–923, https://doi.org/10.1002/dneu.20931.
[6] E. Knight, S. Przyborski, Advances in 3D cell culture technologies enabling tissue-like structures to be created in vitro, J. Anat. 227 (2015) 746–756, https://doi.org/10.1111/joa.12257.
[7] K. Duval, H. Grover, L.-H. Han, Y. Mou, A.F. Pegoraro, J. Fredberg, Z. Chen, Modeling physiological events in 2D vs. 3D cell culture, Physiology 32 (2017) 266–277, https://doi.org/10.1152/physiol.00036.2016.
[8] M. Kapałczyńska, T. Kolenda, W. Przybyła, M. Zajączkowska, A. Teresiak, V. Filas, M. Ibbs, R. Bliźniak, Ł. Łuczewski, K. Lamperska, 2D and 3D cell cultures - a comparison of different types of cancer cell cultures, Arch. Med. Sci. 14 (2018) 910–919, https://doi.org/10.5114/aoms.2016.63743.
[9] C. Jensen, Y. Teng, Is it time to start transitioning from 2D to 3D cell culture? Front. Mol. Biosci. 7 (2020) 33, https://www.frontiersin.org/article/10.3389/fmolb.2020.00033, https://www.frontiersin.org/article/10.3389/fmolb.2020.00033.
[10] J. Jin, S. Tilve, Z. Huang, L. Zhou, H.M. Geller, P. Yu, Effect of chondroitin sulfate proteoglycans on neuronal cell adhesion, spreading and neurite growth in culture, Neural Regen. Res. 13 (2018) 289–297, https://doi.org/10.4103/1673-5374.226398.
[11] H. Rauvala, M. Paveliev, J. Kuja-Panula, N. Kulesskaya, Inhibition and enhancement of neural regeneration by chondroitin sulfate proteoglycans, Neural Regen. Res. 12 (2017) 687–691, https://doi.org/10.4103/1673-5374.206630.
[12] N. George, H.M. Geller, Extracellular matrix and traumatic brain injury, J. Neurosci. Res. 96 (2018) 573–588, https://doi.org/10.1002/jnr.24151.
[13] I. Song, A. Dityatev, Crosstalk between glia, extracellular matrix and neurons, Brain Res. Bull. 136 (2018) 101–108, https://doi.org/10.1016/j.brainresbull.2017.03.003.
[14] E.J. Berns, Z. Álvarez, J.E. Goldberger, J. Boekhoven, J.A. Kessler, H.G. Kuhn, S. I. Stupp, A tenascin-C mimetic peptide amphiphile nanofiber gel promotes neurite outgrowth and cell migration of neurosphere-derived cells, Acta Biomater. 37 (2016) 50–58, https://doi.org/10.1016/j.actbio.2016.04.010.
[15] G.M. Harris, N.N. Madigan, K.Z. Lancaster, L.W. Enquist, A.J. Windebank, J. Schwartz, J.E. Schwarzbauer, Nerve guidance by a decellularized fibroblast extracellular matrix, Matrix Biol. 60–61 (2017) 176–189, https://doi.org/10.1016/j.matbio.2016.08.011.
[16] J.A. Hammarback, S.L. Palm, L.T. Furcht, P.C. Letourneau, Guidance of neurite outgrowth by pathways of substratum-adsorbed laminin, J. Neurosci. Res. 13 (1985) 213–220, https://doi.org/10.1002/jnr.490130115.
[17] A.R. D'Amato, D.L. Puhl, A.M. Ziemba, C.D.L. Johnson, J. Doedee, J. Bao, R. J. Gilbert, Exploring the effects of electrospun fiber surface nanotopography on neurite outgrowth and branching in neuron cultures, PLoS One 14 (2019), e0211731, https://doi.org/10.1371/journal.pone.0211731.
[18] C. Frick, M. Müller, U. Wank, A. Tropitzsch, B. Kramer, P. Senn, H. Rask-Andersen, K.-H. Wiesmüller, H. Löwenheim, Biofunctionalized peptide-based hydrogels provide permissive scaffolds to attract neurite outgrowth from spiral ganglion neurons, Colloids Surf.B Biointerfaces 149 (2017) 105–114, https://doi.org/10.1016/j.colsurfb.2016.10.003.

[19] X. Li, Q. Zhang, Z. Luo, S. Yan, R. You, Biofunctionalized silk fibroin nanofibers for directional and long neurite outgrowth, Biointerphases 14 (2019) 61001, https://doi.org/10.1063/1.5120738.

[20] M.S. Kang, S.-J. Song, J.H. Cha, Y. Cho, H.U. Lee, S.-H. Hyon, J.H. Lee, D.-W. Han, Increased neuritogenesis on ternary nanofiber matrices of PLCL and laminin decorated with black phosphorus, J. Ind. Eng. Chem. 92 (2020) 226–235, https://doi.org/10.1016/j.jiec.2020.09.009.

[21] M. Nomizu, B.S. Weeks, C.A. Weston, W.H. Kim, H.K. Kleinman, Y. Yamada, Structure-activity study of a laminin α1 chain active peptide segment Ile-Lys-Val-Ala-Val (IKVAV), FEBS Lett. 365 (1995) 227–231, https://doi.org/10.1016/0014-5793(95)00475-O.

[22] D.N. Adams, E.Y.-C. Kao, C.L. Hypolite, M.D. Distefano, W.-S. Hu, P.C. Letourneau, Growth cones turn and migrate up an immobilized gradient of the laminin IKVAV peptide, J. Neurobiol. 62 (2005) 134–147, https://doi.org/10.1002/neu.20075.

[23] K. Tashiro, G.C. Sephel, B. Weeks, M. Sasaki, G.R. Martin, H.K. Kleinman, Y. Yamada, A synthetic peptide containing the IKVAV sequence from the a chain of laminin mediates cell attachment, migration, and neurite outgrowth, J. Biol. Chem. 264 (1989) 16174–16182, http://www.jbc.org/content/264/27/16174.abstract, http://www.jbc.org/content/264/27/16174.abstract.

[24] M.C. Kibbey, M. Jucker, B.S. Weeks, R.L. Neve, W.E. Van Nostrand, H.K. Kleinman, Beta-amyloid precursor protein binds to the neurite-promoting IKVAV site of laminin, Proc. Natl. Acad. Sci. U. S. A. 90 (1993) 10150–10153, http://www.ncbi.nlm.nih.gov/pmc/articles/PMC47731/, http://www.ncbi.nlm.nih.gov/pmc/articles/PMC47731/.

[25] A. Farrukh, F. Ortega, W. Fan, N. Marichal, J.I. Paez, B. Berninger, A. del Campo, M.J. Salierno, Bifunctional hydrogels containing the laminin motif IKVAV promote neurogenesis, Stem Cell Rep. 9 (2017) 1432–1440, https://doi.org/10.1016/j.stemcr.2017.09.002.

[26] T.H. Perera, S.M. Howell, L.A. Smith Callahan, Manipulation of extracellular matrix remodeling and neurite extension by mouse embryonic stem cells using IKVAV and LRE peptide tethering in hyaluronic acid matrices, Biomacromolecules 20 (2019) 3009–3020, https://doi.org/10.1021/acs.biomac.9b00578.

[27] P. Liesi, A. Närvänen, J. Soos, H. Sariola, G. Snounou, Identification of a neurite outgrowth-promoting domain of laminin using synthetic peptides, FEBS Lett. 244 (1989) 141–148, https://doi.org/10.1016/0014-5793(89)81180-9.

[28] J.P. Myers, T.M. Gomez, Focal adhesion kinase promotes integrin adhesion dynamics necessary for chemotropic turning of nerve growth cones, J. Neurosci. 31 (2011) 13585 LP–13595, http://www.jneurosci.org/content/31/38/13585.abstract, http://www.jneurosci.org/content/31/38/13585.abstract.

[29] J.P. Myers, E. Robles, A. Ducharme-Smith, T.M. Gomez, Focal adhesion kinase modulates Cdc42 activity downstream of positive and negative axon guidance cues, J. Cell Sci. 125 (2012) 2918–2929, https://doi.org/10.1242/jcs.100107.

[30] R.H. Nichol, T.S. Catlett, M.M. Onesto, D. Hollender, T.M. Gómez, Environmental elasticity regulates cell-type specific RHOA signaling and neuritogenesis of human neurons, Stem Cell Rep. 13 (2019) 1006–1021, https://doi.org/10.1016/j.stemcr.2019.10.008.

[31] H. Bogetofte, P. Jensen, J. Okarmus, S.I. Schmidt, M. Agger, M. Ryding, P. Nørregaard, C. Fenger, X. Zeng, J. Graakjær, B.J. Ryan, R. Wade-Martins, M. R. Larsen, M. Meyer, Perturbations in RhoA signalling cause altered migration and impaired neuritogenesis in human iPSC-derived neural cells with PARK2 mutation, Neurobiol. Dis. 132 (2019), 104581, https://doi.org/10.1016/j.nbd.2019.104581.

[32] A. Rolls, R. Shechter, M. Schwartz, The bright side of the glial scar in CNS repair, Nat. Rev. Neurosci. 10 (2009) 235–241, https://doi.org/10.1038/nrn2591.

[33] J.W. Fawcett, R.A. Asher, The glial scar and central nervous system repair, Brain Res. Bull. 49 (1999) 377–391.

[34] G. Yiu, Z. He, Glial inhibition of CNS axon regeneration, Nat. Rev. Neurosci. 7 (2006) 617–627, https://doi.org/10.1038/nrn1956.

[35] J. Silver, J.H. Miller, Regeneration beyond the glial scar, Nat. Rev. Neurosci. 5 (2004) 146–156, https://doi.org/10.1038/nrn1326.

[36] P.A. Brittis, J.G. Flanagan, Nogo domains and a Nogo receptor: implications for axon regeneration, Neuron 30 (2001) 11–14, https://doi.org/10.1016/S0896-6273(01)00258-6.

[37] M.E. Schwab, Functions of Nogo proteins and their receptors in the nervous system, Nat. Rev. Neurosci. 11 (2010) 799–811, https://doi.org/10.1038/nrn2936.

[38] J. Laurén, F. Hu, J. Chin, J. Liao, M.S. Airaksinen, S.M. Strittmatter, Characterization of myelin ligand complexes with neuronal Nogo-66 receptor family members, J. Biol. Chem. 282 (2007) 5715–5725, https://doi.org/10.1074/jbc.M609797200.

[39] B.P. Liu, A. Fournier, T. GrandPré, S.M. Strittmatter, Myelin-associated glycoprotein as a functional ligand for the Nogo-66 receptor, Science (80-.) 297 (2002) 1190 LP–1193, http://science.sciencemag.org/content/297/5584/1190.abstract.

[40] K.C. Wang, J.A. Kim, R. Sivasankaran, R. Segal, Z. He, p75 interacts with the Nogo receptor as a co-receptor for Nogo, MAG and OMgp, Nature 420 (2002) 74–78, https://doi.org/10.1038/nature01176.

[41] B. Niederost, T. Oertle, J. Fritsche, R.A. McKinney, C.E. Bandtlow, Nogo-A and myelin-associated glycoprotein mediate neurite growth inhibition by antagonistic regulation of RhoA and Rac1, J. Neurosci. 22 (2002) 10368–10376.

[42] S. Mi, X. Lee, Z. Shao, G. Thill, B. Ji, J. Relton, M. Levesque, N. Allaire, S. Perrin, B. Sands, T. Crowell, R.L. Cate, J.M. McCoy, R.B. Pepinsky, LINGO-1 is a component of the Nogo-66 receptor/p75 signaling complex, Nat. Neurosci. 7 (2004) 221–228, https://doi.org/10.1038/nn1188.

[43] A.W. McGee, S.M. Strittmatter, The Nogo-66 receptor: focusing myelin inhibition of axon regeneration, Trends Neurosci. 26 (2003) 193–198, https://doi.org/10.1016/S0166-2236(03)00062-6.

[44] D. Hunt, R.S. Coffin, P.N. Anderson, The Nogo receptor, its ligands and axonal regeneration in the spinal cord; a review, J. Neurocytol. 31 (2002) 93–120, https://doi.org/10.1023/A:1023941421781.

[45] J.B. Park, G. Yiu, S. Kaneko, J. Wang, J. Chang, Z. He, A TNF receptor family member, TROY, is a coreceptor with Nogo receptor in mediating the inhibitory activity of myelin inhibitors, Neuron 45 (2016) 345–351, https://doi.org/10.1016/j.neuron.2004.12.040.

[46] S.T. Wong, J.R. Henley, K.C. Kanning, K. Huang, M. Bothwell, M. Poo, A p75NTR and Nogo receptor complex mediates repulsive signaling by myelin-associated glycoprotein, Nat. Neurosci. 5 (2002) 1302–1308, https://doi.org/10.1038/nn975.

[47] K.C. Wang, V. Koprivica, J.A. Kim, R. Sivasankaran, Y. Guo, R.L. Neve, Z. He, Oligodendrocyte-myelin glycoprotein is a Nogo receptor ligand that inhibits neurite outgrowth, Nature 417 (2002) 941–944, https://doi.org/10.1038/nature00867.

[48] C.E. Ng, B.L. Tang, Nogos and the Nogo-66 receptor: factors inhibiting CNS neuron regeneration, J. Neurosci. Res. 67 (2002), https://doi.org/10.1002/jnr.10134.

[49] J.B. Park, G. Yiu, S. Kaneko, J. Wang, J. Chang, Z. He, A TNF receptor family member, TROY, is a coreceptor with Nogo receptor in mediating the inhibitory activity of myelin inhibitors, Neuron 45 (2005) 345–351, https://doi.org/10.1016/j.neuron.2004.12.040.

[50] J.R. Hull, G.S. Tamura, D.G. Castner, Structure and reactivity of adsorbed fibronectin films on mica, Biophys. J. 93 (2007) 2852–2860, https://doi.org/10.1529/biophysj.107.109819.

[51] D.S. Shah, M.B. Thomas, S. Phillips, D.A. Cisneros, A.P. Le Brun, S.A. Holt, J. H. Lakey, Self-assembling layers created by membrane proteins on gold, Biochem. Soc. Trans. 35 (2007) 522–526, https://doi.org/10.1042/BST0350522.

[52] D. Athey, D.S.H. Shah, S.R. Phillips, J.H. Lakey, A manufacturable surface-biology platform for nano applications; cell culture, analyte detection, diagnostics sensors, Ind. Biotechnol. 1 (2005) 185–189, https://doi.org/10.1089/ind.2005.1.185.

[53] M.J. Cooke, T. Zahir, S.R. Phillips, D.S.H. Shah, D. Athey, J.H. Lakey, M. S. Shoichet, S.A. Przyborski, Neural differentiation regulated by biomimetic surfaces presenting motifs of extracellular matrix proteins, J. Biomed. Mater. Res. A 93 (2010) 824–832, https://doi.org/10.1002/jbm.a.32585.

[54] F. Parker, K. White, S. Phillips, M. Peckham, Promoting differentiation of cultured myoblasts using biomimetic surfaces that present alpha-laminin-2 peptides, Cytotechnology 68 (2016) 2159–2169, https://doi.org/10.1007/s10616-016-0006-y.

[55] M.J. Cooke, S.R. Phillips, D.S.H. Shah, D. Athey, J.H. Lakey, S.A. Przyborski, Enhanced cell attachment using a novel cell culture surface presenting functional domains from extracellular matrix proteins, Cytotechnology 56 (2008) 71–79, https://doi.org/10.1007/s10616-007-9119-7.

[56] K.E. Clarke D.M. Tams A.P. Henderson M.F. Roger A. Whiting S.A. Przyborski A robust and reproducible human pluripotent stem cell derived model of neurite outgrowth in a three-dimensional culture system and its application to study neurite inhibition, Neurochem. Int. (n.d.). doi:10.1016/j.neuint.2016.12.009.

[57] C.C.M. Chan, K. Khodarahmi, J. Liu, D. Sutherland, L.W. Oschipok, J.D. Steeves, W. Tetzlaff, Dose-dependent beneficial and detrimental effects of ROCK inhibitor Y27632 on axonal sprouting and functional recovery after rat spinal cord injury, Exp. Neurol. 196 (2005) 352–364, https://doi.org/10.1016/j.expneurol.2005.08.011.

[58] P.P. Monnier, A. Sierra, J.M. Schwab, S. Henke-Fahle, B.K. Mueller, The Rho/ROCK pathway mediates neurite growth-inhibitory activity associated with the chondroitin sulfate proteoglycans of the CNS glial scar, Mol. Cell. Neurosci. 22 (2003) 319–330.

[59] P. Lingor, N. Teusch, K. Schwarz, R. Mueller, H. Mack, M. Bahr, B.K. Mueller, Inhibition of rho kinase (ROCK) increases neurite outgrowth on chondroitin sulphate proteoglycan in vitro and axonal regeneration in the adult optic nerve in vivo, J. Neurochem. 103 (2007) 181–189, https://doi.org/10.1111/j.1471-4159.2007.04756.x.

[60] J.K. Liao, M. Seto, K. Noma, Rho kinase (ROCK) inhibitors, J. Cardiovasc. Pharmacol. 50 (2007) 17–24, https://doi.org/10.1097/FJC.0b013e318070d1bd.

[61] N. Forgione, M.G. Fehlings, Rho-ROCK inhibition in the treatment of spinal cord injury, World Neurosurg. 82 (2014) e535–e539, https://doi.org/10.1016/j.wneu.2013.01.009.

[62] Y. Fujita, T. Yamashita, Axon growth inhibition by RhoA/ROCK in the central nervous system, Front. Neurosci. 8 (2014), https://doi.org/10.3389/fnins.2014.00338.

[63] M.A. Kopp, T. Liebscher, A. Niedeggen, S. Laufer, B. Brommer, G.J. Jungehulsing, S.M. Strittmatter, U. Dirnagl, J.M. Schwab, Small-molecule-induced rho-inhibition: NSAIDs after spinal cord injury, Cell Tissue Res. 349 (2012) 119–132, https://doi.org/10.1007/s00441-012-1334-7.

[64] Q. Fu, J. Hue, S. Li, Nonsteroidal anti-inflammatory drugs promote axon regeneration via RhoA inhibition, J. Neurosci. 27 (2007) 4154–4164, https://doi.org/10.1523/JNEUROSCI.4353-06.2007.

[65] S. Li, S.M. Strittmatter, Delayed systemic Nogo-66 receptor antagonist promotes recovery from spinal cord injury, J. Neurosci. 23 (2003) 4219 LP–4227, http://www.jneurosci.org/content/23/10/4219.abstract, http://www.jneurosci.org/content/23/10/4219.abstract.

[66] Y. Cao, J.S. Shumsky, M.A. Sabol, R.A. Kushner, S. Strittmatter, F.P.T. Hamers, D. H.S. Lee, S.A. Rabacchi, M. Murray, Nogo-66 receptor antagonist peptide (NEP1-40) administration promotes functional recovery and axonal growth after lateral funiculus injury in the adult rat, Neurorehabil. Neural Repair 22 (2008) 262–278, https://doi.org/10.1177/1545968307308550.

[67] C.C.M. Chan, A.K. Wong, J. Liu, J.D. Steeves, W. Tetzlaff, ROCK inhibition with Y27632 activates astrocytes and increases their expression of neurite growth-

inhibitory chondroitin sulfate proteoglycans, Glia 55 (2007) 369–384, https://doi.org/10.1002/glia.20466.
[68] P. Dergham, B. Ellezam, C. Essagian, H. Avedissian, W.D. Lubell, L. McKerracher, Rho signaling pathway targeted to promote spinal cord repair, J. Neurosci. 22 (2002) 6570 LP–6577, http://www.jneurosci.org/content/22/15/6570.abstract, http://www.jneurosci.org/content/22/15/6570.abstract.
[69] S.M. Gopalakrishnan, N. Teusch, C. Imhof, M.H.M. Bakker, M. Schurdak, D. J. Burns, U. Warrior, Role of rho kinase pathway in chondroitin sulfate proteoglycan-mediated inhibition of neurite outgrowth in PC12 cells, J. Neurosci. Res. 86 (2008) 2214–2226, https://doi.org/10.1002/jnr.21671.
[70] T. Masuda, C. Sakuma, K. Kobayashi, K. Kikuchi, E. Soda, T. Shiga, K. Kobayashi, H. Yaginuma, Laminin peptide YIGSR and its receptor regulate sensory axonal response to the chemoattractive guidance cue in the chick embryo, J. Neurosci. Res. 87 (2009) 353–359, https://doi.org/10.1002/jnr.21868.
[71] X. Yu, G.P. Dillon, R.B. Bellamkonda, A laminin and nerve growth factor-laden three-dimensional scaffold for enhanced neurite extension, Tissue Eng. 5 (1999) 291–304, https://doi.org/10.1089/ten.1999.5.291.
[72] N.O. Dhoot, C.A. Tobias, I. Fischer, M.A. Wheatley, Peptide-modified alginate surfaces as a growth permissive substrate for neurite outgrowth, J. Biomed. Mater. Res.A 71A (2004) 191–200, https://doi.org/10.1002/jbm.a.30103.
[73] J.P. Ranieri, R. Bellamkonda, E.J. Bekos, T.G. Vargo, J.A.J. Gardella, P. Aebischer, Neuronal cell attachment to fluorinated ethylene propylene films with covalently immobilized laminin oligopeptides YIGSR and IKVAV. II, J. Biomed. Mater. Res. 29 (1995) 779–785, https://doi.org/10.1002/jbm.820290614.
[74] E. Agius, Y. Sagot, A.M. Duprat, P. Cochard, Antibodies directed against the β1-integrin subunit and peptides containing the IKVAV sequence of laminin perturb neurite outgrowth of peripheral neurons on immature spinal cord substrata, Neuroscience 71 (1996) 773–786, https://doi.org/10.1016/0306-4522(95)00447-5.
[75] E.J. Berns, S. Sur, L. Pan, J.E. Goldberger, S. Suresh, S. Zhang, J.A. Kessler, S. I. Stupp, Aligned neurite outgrowth and directed cell migration in self-assembled monodomain gels, Biomaterials 35 (2014) 185–195, https://doi.org/10.1016/j.biomaterials.2013.09.077.
[76] R. Bellamkonda, J.P. Ranieri, P. Aebischer, Laminin oligopeptide derivatized agarose gels allow three-dimensional neurite extension in vitro, J. Neurosci. Res. 41 (1995) 501–509, https://doi.org/10.1002/jnr.490410409.
[77] R.Y. Tam, T. Fuehrmann, N. Mitrousis, M.S. Shoichet, Regenerative therapies for central nervous system diseases: a biomaterials approach, Neuropsychopharmacology 39 (2014) 169–188, https://doi.org/10.1038/npp.2013.237.
[78] M. Makino, I. Okazaki, S. Kasai, N. Nishi, M. Bougaeva, B.S. Weeks, A. Otaka, P. K. Nielsen, Y. Yamada, M. Nomizu, Identification of cell binding sites in the laminin alpha5-chain G domain, Exp. Cell Res. 277 (2002) 95–106, https://doi.org/10.1006/excr.2002.5540.
[79] F. Katagiri, M. Ishikawa, Y. Yamada, K. Hozumi, Y. Kikkawa, M. Nomizu, Screening of integrin-binding peptides from the laminin α4 and α5 chain G domain peptide library, Arch. Biochem. Biophys. 521 (2012) 32–42, https://doi.org/10.1016/j.abb.2012.02.017.
[80] M. Nomizu, Y. Kuratomi, S.-Y. Song, M.L. Ponce, M.P. Hoffman, S.K. Powell, K. Miyoshi, A. Otaka, H.K. Kleinman, Y. Yamada, Identification of cell binding sequences in mouse laminin γ1 chain by systematic peptide screening, J. Biol. Chem. 272 (1997) 32198–32205, https://doi.org/10.1074/jbc.272.51.32198.
[81] T. Gordon, Nerve regeneration in the peripheral and central nervous systems, J. Physiol. 594 (2016) 3517–3520, https://doi.org/10.1113/JP270898.
[82] A.K. Varma, A. Das, G. 4th Wallace, J. Barry, A.A. Vertegel, S.K. Ray, N.L. Banik, Spinal cord injury: a review of current therapy, future treatments, and basic science frontiers, Neurochem. Res. 38 (2013) 895–905, https://doi.org/10.1007/s11064-013-0991-6.
[83] A. Sandvig, M. Berry, L.B. Barrett, A. Butt, A. Logan, Myelin-, reactive glia-, and scar-derived CNS axon growth inhibitors: expression, receptor signaling, and correlation with axon regeneration, Glia. 46 (2004) 225–251, https://doi.org/10.1002/glia.10315.
[84] M.D. Benson, M.I. Romero, M.E. Lush, Q.R. Lu, M. Henkemeyer, L.F. Parada, Ephrin-B3 is a myelin-based inhibitor of neurite outgrowth, Proc. Natl. Acad. Sci. U.S.A. 102 (2005) 10694–10699, https://doi.org/10.1073/pnas.0504021102.
[85] J.-K. Sung, L. Miao, J.W. Calvert, L. Huang, H. Louis Harkey, J.H. Zhang, A possible role of RhoA/Rho-kinase in experimental spinal cord injury in rat, Brain Res. 959 (2003) 29–38, https://doi.org/10.1016/S0006-8993(02)03717-4.
[86] A.E. Fournier, B.T. Takizawa, S.M. Strittmatter, Rho kinase inhibition enhances axonal regeneration in the injured CNS, J. Neurosci. 23 (2003) 1416–1423, http://www.jneurosci.org/content/23/4/1416.abstract, http://www.jneurosci.org/content/23/4/1416.abstract.
[87] X. Wu, X. Xu, RhoA/Rho kinase in spinal cord injury, Neural Regen. Res. 11 (2016) 23–27, https://doi.org/10.4103/1673-5374.169601.
[88] Y. Chiba, S. Kuroda, H. Shichinohe, M. Hokari, T. Osanai, K. Maruichi, S. Yano, K. Hida, Y. Iwasaki, Synergistic effects of bone marrow stromal cells and a rho kinase (ROCK) inhibitor, Fasudil on axon regeneration in rat spinal cord injury, Neuropathology 30 (2010) 241–250, https://doi.org/10.1111/j.1440-1789.2009.01077.x.
[89] B.K. Mueller, H. Mack, N. Teusch, Rho kinase, a promising drug target for neurological disorders, Nat. Rev. Drug Discov. 4 (2005) 387–398, https://doi.org/10.1038/nrd1719.
[90] A. Jain, S.M. Brady-Kalnay, R.V. Bellamkonda, Modulation of Rho GTPase activity alleviates chondroitin sulfate proteoglycan-dependent inhibition of neurite extension, J. Neurosci. Res. 77 (2004) 299–307, https://doi.org/10.1002/jnr.20161.